

## ARTICLE OPEN

# Graphene electronic fibres with touch-sensing and light-emitting functionalities for smart textiles

Elias Torres Alonso<sup>1</sup>, Daniela P. Rodrigues<sup>2</sup>, Mukond Khetani<sup>1</sup>, Dong-Wook Shin<sup>1</sup>, Adolfo De Sanctis<sup>1</sup>, Hugo Joulie<sup>1</sup>, Isabel de Schrijver<sup>3</sup>, Anna Baldycheva<sup>1</sup>, Helena Alves<sup>2,4</sup>, Ana I. S. Neves<sup>1</sup>, Saverio Russo<sup>1</sup> and Monica F. Craciun<sup>1</sup>

The true integration of electronics into textiles requires the fabrication of devices directly on the fibre itself using high-performance materials that allow seamless incorporation into fabrics. Woven electronics and opto-electronics, attained by intertwined fibres with complementary functions are the emerging and most ambitious technological and scientific frontier. Here we demonstrate graphene-enabled functional devices directly fabricated on textile fibres and attained by weaving graphene electronic fibres in a fabric. Capacitive touch-sensors and light-emitting devices were produced using a roll-to-roll-compatible patterning technique, opening new avenues for woven textile electronics. Finally, the demonstration of fabric-enabled pixels for displays and position sensitive functions is a gateway for novel electronic skin, wearable electronic and smart textile applications.

*npj Flexible Electronics* (2018)2:25; doi:10.1038/s41528-018-0040-2

## INTRODUCTION

Smart textiles are an emerging research field with applications in medical diagnostics, health monitoring, clothing, home fabrics, automotive textiles, tracking and packaging.<sup>1–3</sup> Devices seamlessly integrated into fabrics represent the ultimate form of smart textiles<sup>4,5</sup> and require the development of fibres endowed with electronic functions. Woven smart textiles attained by intertwined fibres with complementary functions are one of the most ambitious technological and scientific frontiers, which can truly deliver the seamless incorporation of devices into fabrics, with a potential transformative development in intelligent clothing. Such advancements can project wearable electronics to new frontiers whereby the current rigid<sup>6</sup> or semi-flexible<sup>7–13</sup> devices glued onto fabric (e.g. by planarisation layers) will be replaced by electronic fibres coated with imperceptible and low-weight functional components needed to preserve the softness of nowadays clothing. These ambitious aims impose stringent requirements on a vast range of physical properties of the constituent materials, seldom met by most systems typically displaying modest electrical and thermal properties and low chemical stability, leading to poor device performance on fibres.<sup>7,8</sup> The recently discovered atomically thin materials hold the gamut of required properties to develop conceptually novel smart textiles, to include high electrical conductivity,<sup>14–16</sup> optical transparency,<sup>17,18</sup> mechanical strength (with Young's modulus of 2 TPa<sup>19</sup> and fracture strength of 130 GPa<sup>20</sup>), thermal stability<sup>21</sup>, as well as ease of processing into different structures, such as atomically thin-films, paper-like membranes, and printed films. To date, several strategies to integrate graphene materials with textiles have been explored,<sup>9–13,22,23</sup> leading to the development of transistors,<sup>12</sup> supercapacitors<sup>13</sup> and conductive graphene fibres.<sup>22,23</sup> Crucially, woven graphene-enabled textile electronics as well as a pivotal range of opto-electronic technologies such as light-emitting devices and

sensors, essential to enable a ground-breaking development in smart textiles, are still a futuristic theoretical concept.

PP fibres are ubiquitous in textile for numerous applications from healthcare, security and defence to daily life clothing and fabrics. This is due to their wide range of exceptional properties, including the lightest, the lowest thermal conductivity and highest stain resistance than any other fibre. Furthermore, PP fibres also have extreme mechanical flexibility at low temperature and resistance to bacteria, while being recyclable and ecologically friendly. A significant step forward in smart textile would rely on the ability to widen the scope of the PP fibre properties without hampering the features that make this material so special to mankind. Here we demonstrate electronic fibres with functional devices based on graphene directly fabricated on polypropylene (PP) textile fibres typically used in commercial applications. We report two types of electronic devices for future smart textiles: capacitive touch-sensors and light-emitting devices.

Either for leisure, advertising or displaying information, light emitting devices need to be incorporated on textile substrates for truly wearable displays to be achieved. Several examples of such devices on textile fibres have been realised with different electrodes, such as indium tin oxide (ITO), or nanowires (NW), with limitations in terms of stability and flexibility.<sup>24–26</sup> Similarly, several reports of touch-sensors based on different electrodes including graphene have also been published, but most of them have rise and fall times in the order of seconds.<sup>27–30</sup>

To address the device fabrication compatibility with scale-up manufacturing, we developed a roll-to-roll-compatible patterning technique, enabling the integration of graphene circuits into fabrics. By creating woven arrays from such fibres, we demonstrate pixels with different sizes that can be integrated in future textile displays and devices for position sensitive measurements. Our results demonstrating the realisation of fabrics from light-

<sup>1</sup>Centre for Graphene Science, College of Engineering, Mathematics and Physical Sciences, University of Exeter, EX4 4QL Exeter, United Kingdom; <sup>2</sup>Department of Physics and CICECO, University of Aveiro, 3819-130 Aveiro, Portugal; <sup>3</sup>Centexbel, Technologiepark-Zwijinaarde 7, 9052 Ghent, Belgium and <sup>4</sup>Department of Physics, Instituto Superior Técnico, University of Lisbon, Av. Rovisco Pais 1, 1040-001 Lisbon, Portugal  
Correspondence: Monica F. Craciun (M.F.Craciun@exeter.ac.uk)

Received: 24 April 2018 Revised: 24 July 2018 Accepted: 31 July 2018  
Published online: 25 September 2018

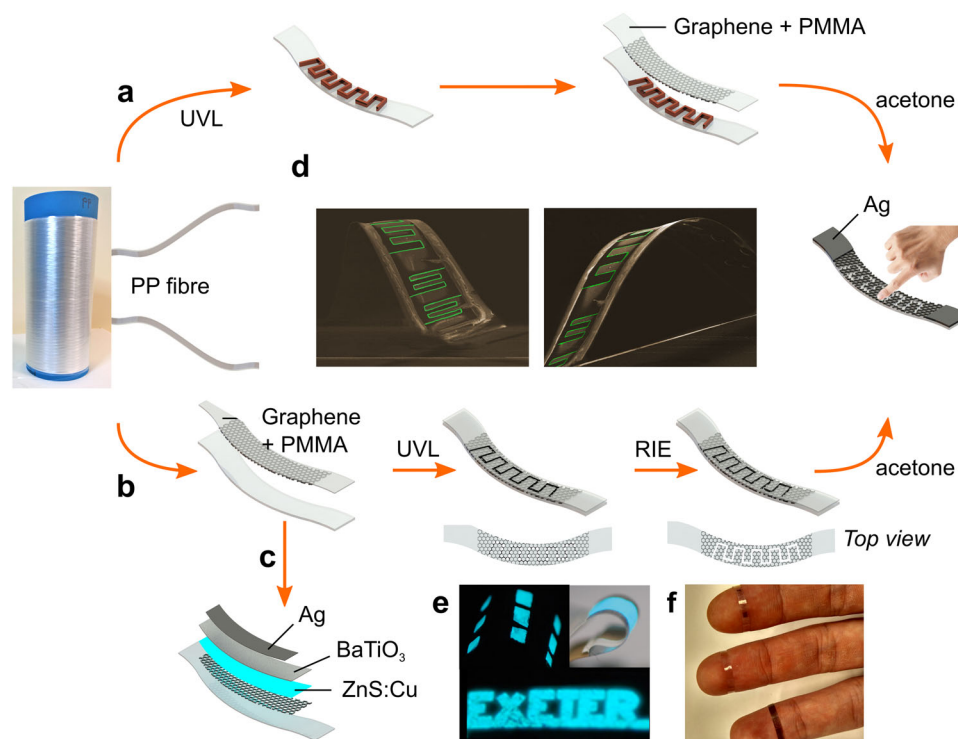


**Fig. 1** Graphene-based devices on textile fibres. Photos of the polypropylene textile fibre; schematics of the step-by-step process to produce touch-sensing devices with a lithography process compatible with roll-to-roll manufacturing **a** and conventional lithography and etching process **b**. SEM pictures of the bent touch sensors are shown in **d** with the gap between graphene electrodes highlighted in green. Schematic and of photos of light emitting devices are shown in **c** and **e**. Photos of touch sensors are shown in **f**

emitting and electronically active fibres usher the development of true smart textiles. To this end, we have developed a non-invasive manufacturing process for electronic PP fibres compatible with industrial processes (Fig. 1 and Methods section). PP fibres were coated with graphene as previously demonstrated.<sup>22,23</sup> For touch-sensing applications, interdigitated electrodes were patterned on the graphene coating using a process compatible with roll-to-roll (R2R) micro-patterning<sup>31</sup> and transfer<sup>32</sup> of graphene on flexible substrates (Fig. 1a), resulting in well-defined patterns down to 50  $\mu\text{m}$  (Fig. 1b and Supplementary Fig. S4). This method leads to better device performance when compared to graphene patterning using reactive ion etching (RIE) (Fig. 1c). Light-emitting devices were fabricated using the graphene coating as electrode in an alternating current electroluminescent (ACEL) configuration<sup>33</sup> (Fig. 1c–e).

The development of graphene in the last decade had a very high pace, which resulted in different methods for the production of graphene of different quality and cost. For example single layer graphene (SLG) and few-layer graphene (FLG) grown by chemical vapor deposition (CVD) represent the best candidates in terms of electronic quality and optical transparency, while liquid phase exfoliated graphene (LEG) is the best candidate in terms of cost, where optical transparency is not a requirement. Choosing the appropriate graphene material for an application is the most critical step to a successful graphene-based flexible and wearable electronics technology. Therefore, in this study we demonstrate the performance of our devices with different types of graphene materials, namely SLG, FLG and LEG. Furthermore, by using different types of graphene we demonstrate that our devices can be produced in a more industrial manufacturing compatible way. For this, we compare graphene grown by CVD (i.e. SLG and FLG with different ranges of conductivity and transparency) to LEG.

## RESULTS

### Capacitive touch sensors

Touch-sensing devices using PP fibres coated with SLG and FLG grown by CVD, and with solution processed graphene films obtained by liquid-exfoliation (LEG) are shown in Figs. 1f and 2a. They were produced using the R2R-compatible method (Fig. 1a). The graphene coatings were characterised by means of Raman spectroscopy (Supplementary Fig. S1, S2 and S3), and optical transmittance (Supplementary Fig. S4a), confirming the presence of the different types of graphene on the surface of the PP textile fibres. Extensive microscopic studies of the surface of graphene-coated fibres along with detailed characterisation of the electrical and optical properties were published in refs. <sup>22,23</sup>. These studies included characterisation techniques, such as atomic force microscopy, scanning electron microscopy, scanning thermal microscopy, surface profilometry, Raman spectroscopy, electrical conductivity measurements, optical transmittance measurements and measurements of the mechanical properties.

There are two main methods of touch-sensing<sup>34</sup>: resistive, where a change in resistance is measured as signal; and capacitive, where this signal comes from a change in capacitance in between the electrodes. We have implemented an approach involving the measurement of the impedance which offers the multi-functionality of switching between resistance and capacitance measurement to detect touch. A polar graph of the impedance is shown in Fig. 2b, with the impedance modulus of 60 M $\Omega$  and the phase  $\varphi = 89^\circ$ , for the untouched device. Upon touching, the modulus reduces by an order of magnitude and the phase drops to  $\varphi = 68^\circ$ , due to the finger shorting the interdigitated electrodes. When the finger is pressed (ON state) the impedance drops, and when released (OFF state) the impedance increases back to its original value with great stability, as can be seen for a FLG device (Fig. 2c). Even for atomically thin graphene active material, the excellent performance of the device is retained upon 500

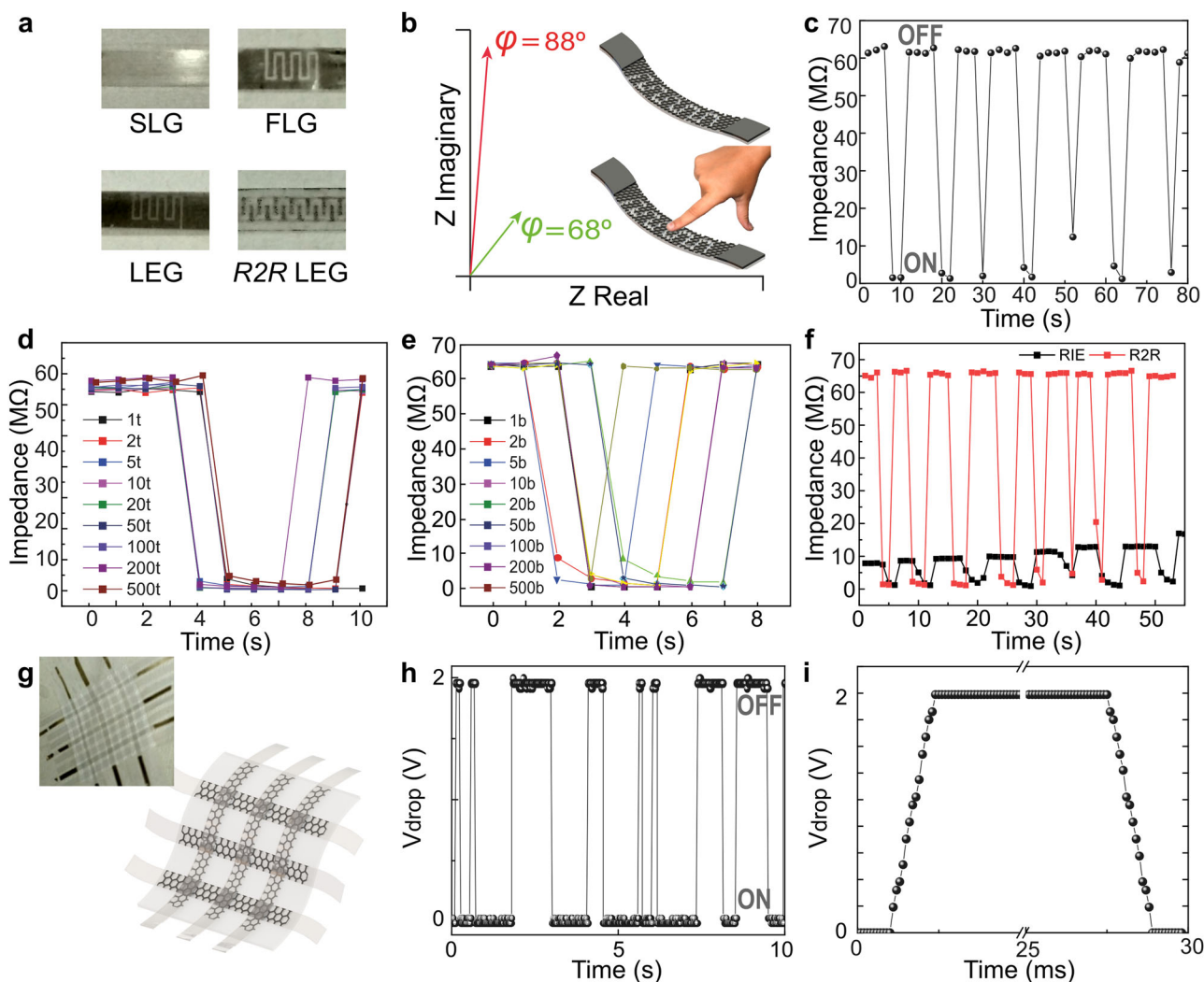


**Fig. 2** Touch sensors: **a** Photographs of sensors with single layer graphene (SLG), few-layer graphene (FLG) fabricated using the roll-to-roll (R2R), solution processed graphene films obtained by liquid-exfoliation blade cut (LEG) and using the R2R compatible method. The LEG sensors using the standard RIE patterning is also shown. **b** Sketch of the impedance response with and without touching. **c** Impedance upon touching versus time for flat FLG device. **d** Impedance upon touching versus time with repeated touching for FLG device. **e** Impedance upon touching versus time with repeated bending for FLG device. **f** Difference in performance between touch sensors patterned using the R2R compatible method and sensors patterned using reactive ion etching (RIE) for LEG. **g** Photo and schematics of position sensitive arrays. **h** Voltage drop upon touching vs. time for position sensitive arrays. **i** Time-resolved rise and fall times upon touching for position sensitive arrays. The various on/off intervals in **c**, **d**, **e**, **f**, **h** are due to the difference in the intensity and duration of the user's finger touching the device

touching cycles, with a clear distinction between the OFF/ON/OFF states (Fig. 2d). We assessed the flexibility of the touch-sensor by subjecting it to mechanical stress and, owing to the exceptional flexibility of graphene, the OFF/ON/OFF device performance remains unchanged upon 500 bends (Fig. 2e). These results are consistent, with great reproducibility (Supplementary Fig. S6 for SLG). To illustrate advantage of our novel R2R approach over standard RIE patterning, we compared it directly with a RIE-based device, as is demonstrated in Fig. 2f, showing that a larger ON/OFF ratio is achieved in the R2R-compatible patterning than in the standard RIE-based method. This is due to the inherently thicker nature of LEG when compared with CVD-grown samples, which makes more difficult to fully remove LEG by RIE. Indeed, after several RIE runs, the films are still conductive in the OFF state, meaning that the graphene was not been fully etched away using RIE. Moreover, the resistance increases after every touch, which is an indication that with every touch the finger is removing graphene flakes from the channel, hence erasing percolation pathways and changing the conductivity of the sample. This

inhomogeneity makes it less suitable for sensor purposes. This effect is not shown in LEG with R2R approach because the photoresist prevented graphene deposition. An even simpler and more scalable method was also shown, using blade-cutting to define the pattern, with results comparable with the R2R method (Supplementary Fig. S7).

Transparent and flexible position-sensitive arrays of graphene-coated fibres were woven in a squared fabric by orthogonally intertwining conducting fibres separated by a poly(methyl methacrylate) (PMMA) dielectric layer, thus providing sensitive points at their intersections (Fig. 2g). The sensing mechanism, in this case, is purely self-capacitive, widely used across the electronics industry (Supplementary section S3). The touch-sensing performance, quantified as the voltage drop across the PMMA layer sandwiched between 2 orthogonal graphene fibres, is shown in Fig. 2h, with very stable ON/OFF states upon several touches. We analysed the speed of sensing (Fig. 2i) and found a rise and fall times of 1.4 ms regardless the type of graphene used. The rise and fall time of our devices are limited by the electronics

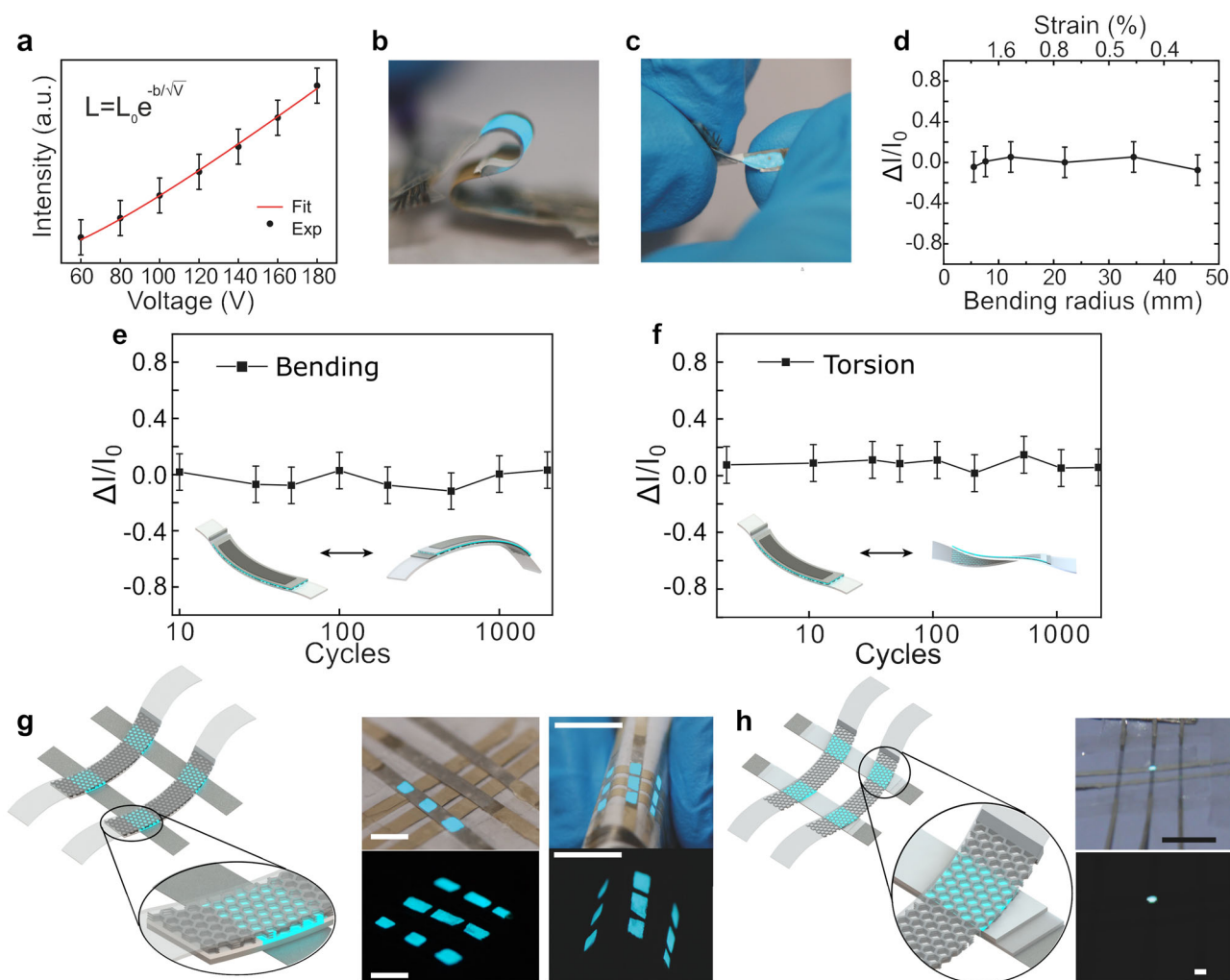


**Fig. 3** ACEL devices on textile fibres: **a** Intensity of the emitted light as a function of bias voltage fitted to the Alfrey–Taylor relation between ACEL brightness ( $L$ ) and voltage ( $V$ ):  $L = L_0 \exp(-b/V)^{1/2}$ , where  $L_0$  and  $b$  are empirical constants, fitted with the with good agreement ( $R^2 = 0.9982$ ).<sup>34,35</sup> Photograph of the device in bending **b** and torsion **c**. Change in emission as a function of: **d** the bending radius and corresponding fibre strain; **e** repeated bending cycles; **f** repeated twisting cycles. Two approaches to ACEL arrays and corresponding photos in light and dark conditions: **g** large pixels (scale bars: left 5 mm; right 20 mm) and **h** small pixels (scale bars: top 10 mm; bottom 1 mm)

used in the measurement, within the range of commercial devices and rival with the best values in the literature.<sup>27–30</sup> In contrast to miniaturised conventional CMOS electronics that are mounted on flexible and textile substrates,<sup>35</sup> smart textiles attained by intertwined graphene fibres allow advanced detection schemes that can be readily implemented when complex functions such as simultaneous multi-touch features are required (Supplementary Video 1).

#### Light-emitting devices

Having demonstrated a novel technology for enabling sensing capabilities of PP fibres, we now proceed to considerably broaden the spectrum of applications by describing the development of graphene-enabled textile fibres with light-emitting functionalities and woven opto-electronic technologies. The ACEL device configuration was chosen as this technology uniquely enables the realisation of large-area flexible and foldable graphene light sources, with good contrast and uniform brightness.<sup>33</sup> Furthermore, ACEL devices can display images with high resolution, can withstand mechanical shocks and a wide range of temperatures,<sup>36</sup> making this technology a valuable candidate for smart textiles. ACEL devices were fabricated on individual graphene-coated PP fibres which served as bottom electrode. Graphene was

subsequently covered by an emitter layer of commercially available Cu-doped zinc sulfide (ZnS:Cu), an insulating layer of BaTiO<sub>3</sub> and a top electrode (Fig. 1c, e). Further details about the coating techniques and optimisation of the devices can be found in Supplementary section S5 and Fig. S10–12 therein. Upon excitation with an AC voltage, light is emitted from the ZnS:Cu layer due to impact ionisation and recombination of electron-hole pairs.<sup>37</sup> The emission spectra is in the visible, with an emission peak around 500 nm (Supplementary Fig. S11) and average light intensity dependent on the applied voltage, as typical for ACEL devices (Fig. 3a).<sup>30</sup> Figures 1e and 3b, c show photos of light-emitting devices on individual fibres, as well as text displayed on fibre achieved by patterning the graphene electrode with features down to 100 μm.

To ascertain the mechanical properties of the light-emitting textile fibres we have subjected the fibres to different types of mechanical stress such as bending, torsion and cyclic loading, assessing the changes in the average intensity ( $\Delta I$ ) as compared to the average light intensity before applying the stress ( $I_0$ ). As shown in Fig. 3d, the change in emission upon bending was negligible up to a 10 mm radius, similar to the radius of a human finger. The mechanical resilience of the device was studied in the form of repeated bending (Fig. 3b, e) and torsion tests (Fig. 3c, f)

between the flat state and the bent or twisted state. For both types of stress, only slight changes were observed, demonstrating the suitability of these devices for smart textile technology.

Finally, to demonstrate the potential of light-emitting textile fibres for fabric-enabled pixels for displays, we fabricated arrays of light-emitting fibres. Two types of arrays were built: (1) fibres coated with graphene electrode, ZnS:Cu and BaTiO<sub>3</sub>, with large pixels ( $\approx 6 \text{ mm}^2$ ) at the intersection with orthogonal silver-coated fibres (Fig. 3g); and (2) fibres coated with silver, ZnS:Cu and BaTiO<sub>3</sub>, with smaller pixels ( $0.25 \text{ mm}^2$ ) at the intersection with fibres with graphene (Fig. 3h). Both device configurations have high performance in terms of light intensity and mechanical properties, similar to the light-emitting fibres presented in Fig. 3a–f. This illustrates the possibility of creating individual pixels and to scale the size of the pixels down without changing the approach.

## DISCUSSION

In summary, we have demonstrated transparent, flexible and durable graphene-enabled touch-sensors and light-emitting devices completely integrated on textile fibres. Both types of wearable sensors were fabricated using methods that are compatible with roll-to-roll and printing techniques, highlighting the potential for these to be scaled up and meet industry requirements. We also verified that the touch sensors patterned using a roll-to-roll-compatible process outperform those fabricated with conventional lithography. We have fabricated arrays of both types of devices to show that these devices can be integrated in a woven fabric. The resulting intertwined devices can be used for fully flexible and highly sensitive position sensors and displays with different pixel sizes.

Our results constitute a new step towards the realisation of electronics directly into textile, and open new possibilities for the use of smart textiles in many applications, such as electronic skin and wearable electronics.

## METHODS

### Graphene production

SLG was grown by chemical vapour deposition on Cu, using a furnace (MTI Instruments) with a quartz tube. After the Cu is placed in a crucible, the system is pumped down and flush with Ar to remove oxygen. After ramping up the temperature ( $33^\circ/\text{min}$ ) up to  $1000^\circ\text{C}$ , the Cu is annealed under an Ar/H<sub>2</sub> atmosphere to remove native oxides and increase grain size. Upon introduction of CH<sub>4</sub>, graphene growth is started and maintained for 15 min. After that, CH<sub>4</sub> is switched off and the furnace is let to cool down to room temperature under Ar flow. Few-layer graphene (FLG) on Ni was purchased (Graphene Supermarket). Liquid-exfoliated graphene (LEG) was produced by shear exfoliation of graphite powder (Graphene Supermarket). Graphite powder was suspended in water and stabilised with the help of sodium cholate (Sigma-Aldrich). It was blended for 2 h at 6000 rpm with an L5 High Shear Mixer (Silverson Ltd), centrifuged for an hour at 8000 rpm, and then decanted.

### Graphene transfer

Improved graphene adhesion can be achieved by subjecting the fibres to a mild oxygen plasma or to ultraviolet light in the presence of oxygen, prior to the graphene transfer. This increases hydrophilicity. SLG and FLG were transferred to the PP fibres as previously described.<sup>23</sup> The fibres were rinsed in acetone and isopropanol. LEG suspensions were filtered on a cellulose membrane. This membrane was dipped in water, placed on top of the fibre and dry gun from the backside, releasing the graphene film. This process was repeated 2–3 times to ensure conductive films. Raman spectra of the PP fibres before and after the graphene coating are given in Supplementary Fig. S1, with details around the G peak area in Supplementary Fig. S2, denoting the presence of graphene. Raman of the same types of graphene on SiO<sub>2</sub> are shown in Supplementary Fig. S3.

**Textile fibres.** Tape-shaped polypropylene (PP, 0.03 mm thick and 2.4 mm wide) fibres were produced by Centexbel using a monofilament extrusion line, reeled onto a bobbin and cut to the desired length.

### Touch-sensors

Aiming at a scalable manufacturing of these devices, we developed a process which is compatible with roll-to-roll fabrication. In this method (route (a) in Fig. 1) a photoresist layer is deposited on the fibre and patterned prior to the deposition of graphene. The photoresist, together with the supporting PMMA layer used for the transfer of CVD graphene, was simultaneously removed with acetone. This resulted in an effective transfer of the pattern to all the graphene materials used to coat the PP fibres. Well-defined interdigitated electrodes with features ranging from  $100 \mu\text{m}$  down to  $50 \mu\text{m}$  wide and pitch from  $1000 \mu\text{m}$  of  $250 \mu\text{m}$  are shown in Supplementary Fig. S5.

### Light-emitting devices

Graphene was contacted with silver paint and dried in air at  $75^\circ\text{C}$ . ZnS:Cu and BaTiO<sub>3</sub> were purchased from DuPont Inc., spun at 2000 and 3500 rpm, respectively, and dried in air at  $75^\circ\text{C}$ . Silver paint was used for the rear contact.<sup>26</sup> Despite the inherent roughness of the fibres (Supplementary Fig. S8), these light-emitting devices are easily fabricated by spin coating (surface analysis and emission spectra in Supplementary Figs. S9–S12), with compatibility with screen-printing and roll-to-roll processes, allowing also for a possible encapsulation due to the planar nature of the materials and the resulting devices.

### Patterning

UV-lithography was performed by means of a laser-writer (Microwriter ML from Durham Magneto Optics Ltd). The graphene was coated with Microposit S1813 photoresist (MicroChem Corp.) and baked for 60 s at  $120^\circ\text{C}$ . The resist was developed with MF-319 developer (MicroChem Corp.) and immersed in DI water to stop the developing. Then the samples were introduced into a JLS Reactive Ion Etching to perform an O<sub>2</sub> plasma (4 min at 20 W for the ACEL devices and 30 s at 30 W for the touch-sensors) to remove the graphene.

### Optical, thermal and electrical characterisation

The light-emitting devices were powered with an ELD-250 Interfer from ENZ electronics. The emission was collected through an Olympus BXiS microscope mounted with an Olympus MPLFLN lens attached to an ACTON-SP2500 spectrometer (1800 g/mm, 500 nm Blaze) with a PIXIS 2KB eXcelon CCD. Raman, transmittance and light emission spectroscopy were performed using a custom-built setup<sup>38</sup> based on an Olympus coupled to Princeton Instruments ACTON-SP2500 spectrometer (1800 g/mm, 500 nm Blaze) with a PIXIS-400 eXcelon CCD. The optics was calibrated with an IntelliCall<sup>®</sup> calibration source. The impedance was measured with a HM8118 LCR Bridge (Rohde & Schwarz). The position sensing arrays and devices were measured with a commercial PICkit Analyzer (MicroChip Technology Inc), a commercially available Charge Time Measurement Unit (CTMU) microcontroller and an algorithm to recognise the touch (Supplementary section on Position-sensitive arrays).

### Additional characterisation

Fibre profiles and spin coating thickness data were acquired with an AlphaStep<sup>®</sup> D-500 Stylus profiler from KLA Tencor Corp. Raman Spectra was taken with a inVia Raman microscope from Renishaw Plc. SEM images were acquired with a Hitachi SU-70 scanning electron microscope at an accelerating voltage of 4 kV, working distance of  $6200 \mu\text{m}$ , emission current of 44,000 nA, and magnifications of  $\times 100$ ,  $\times 200$ ,  $\times 500$ ,  $\times 1000$  and  $\times 10,000$ .

## DATA AVAILABILITY

The authors declare that all relevant data are included in the paper and in Supplementary Information files.

## ACKNOWLEDGEMENTS

We acknowledge financial support from: the European Commission (H2020-MSCA-IF-2015-704963 and FP7-ICT-2013-613024-GRASP), the European Union Erasmus+ programme, the UK Engineering and Physical Sciences Research Council (EPSRC) (Grants no. EP/K017160/1, EP/K010050/1, EP/M001024/1, EP/M002438/1), the Royal Society international Exchanges Scheme 2016/R1, the Leverhulme Trust (Grant "Quantum Revolution"), the Portuguese Foundation for Science and Technology (FCT), co-financed by FEDER (PT2020 Partnership Agreement), under contracts IF/01088/2014, BI/UI89/2015, and POCI-01-0145-FEDER-007679 (Ref. UID/CTM/50011/2013).

## AUTHOR CONTRIBUTIONS

M.F.C., S.R. and E.T.A. conceived the devices. E.T.A. fabricated and characterised the devices, with D.P.R. and A.B. contributing for the SEM imaging, M.K. and E.T.A. for the touch-sensing p-cap array measurements, A.D.S. for the transmittance measurements and D.-W.S. and W.T.A. for the liquid exfoliation and transfer. H.J. produced the sketches and schemes. I.d.S. fabricated the textile fibres. A.I.S.N. and E.T.A. wrote the manuscript. A.B., H.A., A.I.S.N., S.R. and M.F.C. supervised the project. All the authors discussed the results and commented on the manuscript.

## ADDITIONAL INFORMATION

**Supplementary information** accompanies the paper on the *npj Flexible Electronics* website (<https://doi.org/10.1038/s41528-018-0040-2>).

**Competing interests:** The authors declare no competing interests.

**Publisher's note:** Springer Nature remains neutral with regard to jurisdictional claims in published maps and institutional affiliations.

## REFERENCES

- Schneegass, S., Amft, O. (eds). *Smart Textiles – Human-Computer Interaction Series*. (Springer, Cham, 2017).
- Weng, W. et al. Smart electronic textiles. *Angew. Chem. Int. Ed.* **55**, 6140–6169 (2016).
- Flcury, A., Sugar, M. & Chau, T. E-textiles in clinical rehabilitation: a scoping review. *Electronics* **4**, 173–203 (2015).
- Tao, X. et al. How to make reliable, washable, and wearable textronic devices. *Sensors* **17**, 673 (2017).
- Zeng, W. et al. Fiber-based wearable electronics: a review of materials, fabrication, devices, and applications. *Adv. Mater.* **26**, 5310–5336 (2014).
- Stoppa, M. & Chiolerio, A. Wearable electronics and smart textiles: a critical review. *Sensors* **14**, 11957–11992 (2014).
- Lebedev, V. et al. Investigation of sensing capabilities of organic bi-layer thermistor in wearable e-textile and wireless sensing devices. *Org. Electron.* **42**, 146–152 (2017).
- Zhang, Z. et al. A colour-tunable, weavable fibre-shaped polymer light-emitting electrochemical cell. *Nat. Photonics* **9**, 233–238 (2015).
- Molina, J. Graphene-based fabrics and their applications: a review. *RSC Adv.* **6**, 68261–68291 (2016).
- Meng, F. et al. Graphene-based fibers: a review. *Adv. Mater.* **27**, 5113–5131 (2015).
- Cao, J. & Wang, C. Multifunctional surface modification of silk fabric via graphene oxide repeatedly coating and chemical reduction method. *Appl. Surf. Sci.* **405**, 380–388 (2017).
- Carey, T. et al. Fully inkjet-printed two-dimensional material field-effect heterojunctions for wearable and textile electronics. *Nat. Commun.* **8**, 1202 (2017).
- Abdelkader, A. M. et al. Ultraflexible and robust graphene supercapacitors printed on textiles for wearable electronic applications. *2D Mater.* **4**, 035016 (2017).
- Khrapach, I. et al. Novel highly conductive and transparent graphene-based conductors. *Adv. Mater.* **24**, 2844–2849 (2012).
- Wehenkel, D. J. et al. Unforeseen high temperature and humidity stability of FeCl<sub>3</sub> intercalated few layer graphene. *Sci. Rep.* **5**, 7609 (2015).

- Bointon, T. H., Barnes, M. D., Russo, S. & Craciun, M. F. High quality monolayer graphene synthesized by resistive heating cold wall chemical vapor deposition. *Adv. Mater.* **27**, 4200–4206 (2015).
- Bointon, T. H. et al. Large-area functionalized CVD graphene for work function matched transparent electrodes. *Sci. Rep.* **5**, 16464 (2015).
- Nair, R. R. et al. Fine structure constant defines visual transparency of graphene. *Science* **320**, 1308–1308 (2008).
- Lee, J., Yoon, D. & Cheong, H. Estimation of Young's modulus of graphene by Raman spectroscopy. *Nano Lett.* **12**, 4444–4448 (2012).
- Lee, C., Wei, X., Kysar, J. W. & Hone, J. Measurement of the elastic properties and intrinsic strength of monolayer graphene. *Science* **321**, 385–388 (2008).
- Bolotin, K. I. et al. Ultrahigh electron mobility in suspended graphene. *Solid State Commun.* **146**, 351–355 (2008).
- Neves, A. I. S. et al. Transparent conductive graphene textile fibres. *Sci. Rep.* **5**, 09866 (2015).
- Neves, A. I. S. et al. Towards conductive textiles: coating polymeric fibres with graphene. *Sci. Rep.* **7**, 4250 (2017).
- Yang, H., Lightner, C. R. & Dong, L. Light-emitting coaxial nanofibers. *ACS Nano*. **6**, 622–628 (2012).
- Wang, J., Yan, C. & Chee, K. J. Highly stretchable and self-deformable alternating current electroluminescent devices. *Adv. Mater.* **27**, 2876–2882 (2015).
- Choi, S. et al. Highly flexible and efficient fabric-based organic light-emitting devices for clothing-shaped wearable displays. *Sci. Rep.* **7**, 6424 (2017).
- Chun, S., Kim, Y., Jung, H. & Park, W. A flexible graphene touch sensor in the general human touch range. *Appl. Phys. Lett.* **105**, 041907 (2014).
- Lee, X. et al. Flexible graphene woven fabrics for touch sensing. *Appl. Phys. Lett.* **102**, 163117 (2013).
- Jeong, Y. R. et al. Highly stretchable and sensitive strain sensors using fragmented graphene foam. *Adv. Func. Mater.* **25**, 4228–4236 (2015).
- Chun, S. et al. A graphene force sensor with pressure-amplifying structure. *Carbon* **78**, 601–608 (2014).
- Ahn, S. H. & Guo, L. J. High-speed roll-to-roll nanoimprint lithography on flexible plastic substrates. *Adv. Mater.* **20**, 2044–2049 (2008).
- Bae, S. et al. Roll-to-roll production of 30-inch graphene films for transparent electrodes. *Nat. Nanotechnol.* **5**, 574–578 (2010).
- Torres Alonso, E. et al. Homogeneously bright, flexible, and foldable lighting devices with functionalized graphene electrodes. *ACS Appl. Mater. Interfaces* **8**, 16541–16545 (2016).
- Humza, A., Kemao, Q. & Kakarala, R. A review of touch sensing technologies for small and large-scale touch panels. *Proc. SPIE* **10449**, 1044918 (2017).
- Heidari, H., Nunez, C. G. & Dahiya, R. E-Skin Module with Heterogeneously Integrated Graphene Touch Sensors and CMOS Circuitry. *IEEE Sensors* (2016).
- Wang, Z.-g et al. Flexible graphene-based electroluminescent devices. *ACS Nano* **5**, 7149–7154 (2011).
- Bredol, M. & Dieckhoff, H. S. Materials for powder-based AC-electroluminescence. *Materials* **3**, 1353–1374 (2010).
- De Sanctis, A. et al. An integrated and multi-purpose microscope for the characterization of atomically thin optoelectronic devices. *Rev. Sci. Instrum.* **88**, 055102 (2017).



**Open Access** This article is licensed under a Creative Commons Attribution 4.0 International License, which permits use, sharing, adaptation, distribution and reproduction in any medium or format, as long as you give appropriate credit to the original author(s) and the source, provide a link to the Creative Commons license, and indicate if changes were made. The images or other third party material in this article are included in the article's Creative Commons license, unless indicated otherwise in a credit line to the material. If material is not included in the article's Creative Commons license and your intended use is not permitted by statutory regulation or exceeds the permitted use, you will need to obtain permission directly from the copyright holder. To view a copy of this license, visit <http://creativecommons.org/licenses/by/4.0/>.

© The Author(s) 2018